Earth and Space Science

METHOD
10.1029/2021EA002205

Key Points:

- *b* maps
- Free parameter method
- Independence of the *b* values

Supporting Information:

Supporting Information may be found in the online version of this article.

Correspondence to:

C. Godano,
cataldo.godano@unicampania.it

Citation:

Godano, C., Convertito, V., Pino, N. A., & Tramelli, A. (2022). An automated method for mapping independent spatial *b* values. *Earth and Space Science*, *9*, e2021EA002205. https://doi.org/10.1029/2021EA002205

Received 26 DEC 2021
Accepted 13 MAY 2022

Author Contributions:

Conceptualization: C. Godano, V. Convertito, N. A. Pino, A. Tramelli
Data curation: C. Godano, V. Convertito, N. A. Pino, A. Tramelli
Formal analysis: C. Godano, V. Convertito, N. A. Pino, A. Tramelli
Software: C. Godano
Writing – original draft: C. Godano, V. Convertito, N. A. Pino, A. Tramelli
Writing – review & editing: C. Godano, V. Convertito, N. A. Pino, A. Tramelli

An Automated Method for Mapping Independent Spatial *b* Values

C. Godano[1,2], V. Convertito[2], N. A. Pino[2], and A. Tramelli[2]

[1]Department of Mathematics and Physics, Università della Campania—Luigi Vanvitelli, Caserta, Italy, [2]Istituto Nazionale di Geofisica e Vulcanologia—Sezione di Napoli Osservatorio Vesuviano, Napoli, Italy

Abstract We present an automated method for mapping the *b* values. The algorithm is very simple and presents three advantages: (a) it does not requires any tuning of the parameters like, for instance, a fixed cell size or a maximum radius of the cell; (b) it implies a more appropriate use of the catalog, by using almost all the events in the catalog used (with a tolerance of 1%) with no overlap; (c) it implies the full independence of the *b* values, thus allowing the statistical comparison of the results using standard tests. Although the resulting *b* values are comparable with those obtained by applying the other methods of common use in seismology, these latter (a) leave out many earthquakes from the analysis, with loose of useful information, (b) produce diffuse cells overlapping aiming at reaching many cells of the grid in order to get the correct number of events in each cell, and (c) results in correlated *b* values, which do not allow the test of significance for the differences in the *b* values. Finally, due to the independence from any ad hoc a-priori choice, our method is suitable for automatic and operator-free procedures.

Plain Language Summary The methods usually used in seismology for mapping the *b* value require the tuning of some parameters depending on the analyzed catalog. Here we propose a method that only implies the choice of the minimum number of earthquakes needed to obtain reliable *b* value estimates, which does not depend on the specific cases. Due to the mutual complete independence of the resulting *b* values, the proposed method allows the use of standard statistical tests to compare the results.

1. Introduction

The frequency/magnitude distribution of earthquakes is described by the well known Gutenberg and Richter law (Gutenberg & Richter, 1944) law

$$\log N = a - b(m - m_c) \tag{1}$$

where N is the number of earthquakes with magnitude larger than m, a and b represent a productivity and a scaling parameter. m_c is the completeness magnitude, namely the lowest magnitude at which all the earthquakes, occurring in a certain region and in a given time window, are detected and reported in the earthquake catalog (Rydelek & Sacks, 1989). The completeness magnitude is a crucial variable: when underestimated, it could cause a bias in the *b* value estimation; whereas would narrow the magnitude range of the suitable earthquakes, leaving too few events to calculate any *b* value or resulting in a larger standard deviation, with both cases implying a loss of information.

The *b* parameter has been extensively studied using recorded earthquake catalogs and in laboratory experiments and its value has been associated to the rheological and physical parameters of the medium, being inversely correlated to stress state (Amitrano, 2003; Gulia & Wiemer, 2010; Scholz, 1968; Wyss, 1973) and directly correlated to the thermal gradient (Warren & Latham, 1970; Wiemer et al., 1998) and to the material heterogeneity (Mogi, 1962). Also major events such as magma intrusions or the occurrence of large earthquakes can change *b* locally (Wiemer et al., 1998; Wyss et al., 1997). Time variations of the *b* value have also been used to discriminate between foreshocks and mainshocks in seismic sequences (Gulia & Wiemer, 2019) possibly allowing time dependent seismic hazard assessment.

Different criteria are adopted to map the *b* value over extended areas. In general, maps are usually evaluated by grouping earthquakes in space and/or time and determining a single *b* value for each set. In some investigations, the earthquakes are grouped according to the faulting style and a single *b* values is determined for each

Table 1
The Areas, the Minimum and Maximum Latitude and Longitude, the Initial and Final Dates and the Number of Earthquakes $\mathcal{N}$ in Each Catalog

Area	Lon_{min}	Lon_{max}	Lat_{min}	Lat_{max}	Start date	End date	$\mathcal{N}$
Greece	19.5	28.0	35.0	42.99	1995/1/1	2020/10/30	90,501
Italy	5.28	20.0	35.0	48.3	2003/1/1	2019/3/29	335,231
California	−121.16	−112.79	29.98	38.13	1981/1/1	2019/12/31	699,175
New Zealand	−49.13	−32.29	164.11	180.64	1996/2/29	2020/1/1	413,361

homogeneous area (e.g., Gulia and Wiemer 2010). More often, 2D or 3D maps are developed by suitably gridding the space (e.g., Wiemer and Wyss 1997; Wiemer and Wyss 2002). In these cases, the most commonly used approach is to grid the space into constant size cells and select the earthquakes according to some rules (minimum number of events, maximum distance from the center of the cell, etc.).

Some authors weight each earthquake on the basis of the distance from the node. This method, first introduced by Tormann et al. (2014), has been modified and applied to several regions of the world by many authors (e.g., Kamer and Hiemer, 2015; Taroni et al., 2021; García-Hernández et al., 2021).

In this study we introduce an automated method for spatial gridding with also aiming at avoiding overlapping and the omission of earthquakes that occur when using constant gridding methods. Our method also presents the great advantage that no parameter has to be tuned in advance and it only requires the choice of the number of events per cell. Such an advantage makes the procedure not operator-dependent and, as a consequence, it is well suited to use in seismic surveillance systems.

Finally, we describe the application of our method to four sample areas and also compare the results to the ones obtained for the same areas by other researchers using different methods for spatial gridding.

2. Data and the Automated Gridding Method

2.1. The Analyzed Catalogs

We have focused our study on four different areas of the world: Greece, Italy, New Zealand, and South California. Indeed these areas share a high earthquake occurrence rate and a good quality catalog covering a wide time window. The web sites from where we have downloaded the earthquakes catalog and the names of the institution making available the catalogs are: Italy (INGV, cnt.rm.ingv.it), South California (SCEDC, scedc.caltech.edu/research-tools/altcatalogs.html), Greece (AUTH, http://geophysics.geo.auth.gr/ss/catalogs_en.html, New Zealand (GeoNet, https://www.geonet.org.nz/data/types/eq_catalogue). The minimum and maximum longitude and latitude, with the initial and ending dates and the number of earthquakes in each catalog can be found in Table 1.

Only earthquakes with hypocentral depth smaller than 50 km are included in our analysis. This excludes from the analysis the seismicity occurring in possible slab zones.

2.2. The Algorithm

In estimating the b value, the earthquakes can be grouped by using different strategies. The simplest one is to grid the space in cells of fixed angle Δ in latitude and longitude. Thus the completeness magnitude m_c and the b values are estimated for the events enclosed in each cell. This approach leads to a non uniform distribution of the number of earthquake per cell n_c producing a non uniform distribution of the b value estimation. This could also be ed also by a misevaluation of m_c, as could occur at the margins of a seismic network (for instance, in marine areas), because of the limited data set. Figure S1 in Supporting Information S1 shows the n_c distribution for different values of Δ, for the areas considered here. The distribution $n(n_c)$, the number of cells enclosing n_c events, can be associated to a power law for all the four areas, although if only in the range $100 < n_c < 1{,}000$.

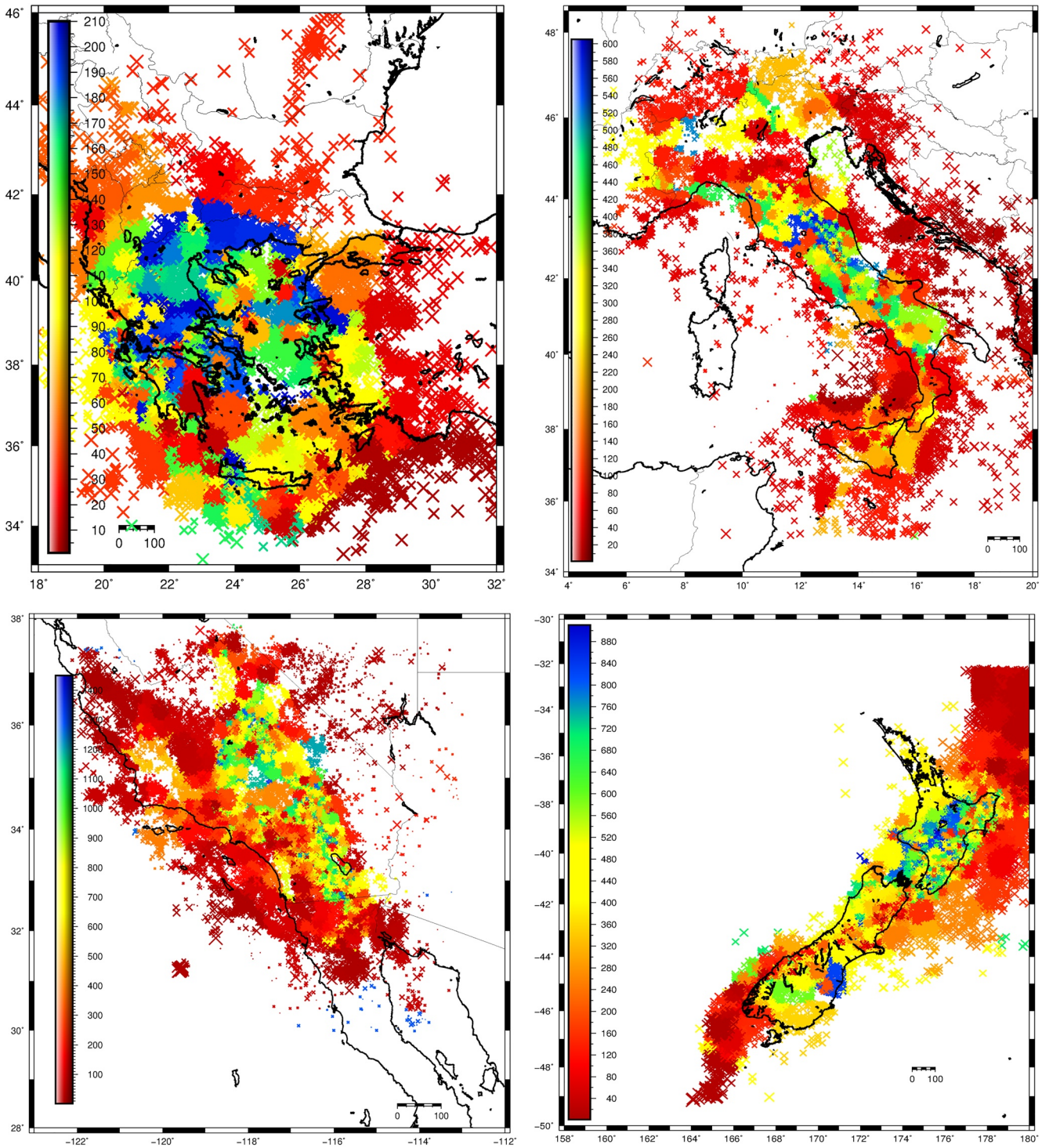

Figure 1. The map of the earthquakes' epicenters colored on the basis of the cell index for the four catalogs here analyzed. All the earthquakes belonging to the same cell assume the same color accordingly to the index of the cell.

This results in a very high variability of n_c invalidating the spatial variability of m_c and b which could be actually induced by the n_c variability. Indeed the b value tends to exhibit large fluctuations with n_c, for small values of n_c (Nava et al., 2017; Tramelli et al., 2021).

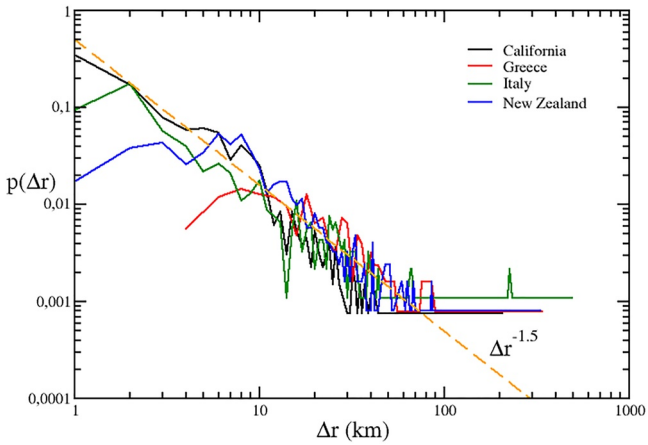

Figure 2. The distribution of the cell size Δr for all the catalogs here analyzed. $p(\Delta r)$ have been opportunely rescaled (the scaling factors are: 1 for California, 1.64 for Greece, 1.56 for Italy and 1.68 for New Zealand) in order to obtain a collapse on a unique master curve, whereas the Δr values have not been changed. The dashed line is plotted as a guide for the eyes.

A different approach consists in the spatial gridding with constant number of events per cell. However, generally this leads to the omission of some events or to the overlapping of contiguous cells reflecting into a not-independent estimation of the b values. This could imply the existence of non trivial spatial correlations between the estimated b values.

A third approach consists into considering the contribution to each cell of all the earthquakes in the catalog weighted with a kernel (generally exponential) depending on the distance of the earthquake from the node of the grid (Tormann et al., 2014).

In order to obtain uniform distribution for n_c on non overlapping cells we introduce a parameter-free gridding method based on an equal number of earthquakes and forcing the inclusion of each earthquake of the catalog in only one cell. In particular we adopt the following algorithm:

1. Fix a distance δ
2. Select the largest event in the catalog (let us call it the ith earthquake)
3. All the earthquakes with a distance from the ith event smaller than δ are included in the cell
4. If the number of the events in the cell is smaller than 500−50, δ is increased by a quantity $\delta_k = k\langle\delta_a\rangle$, where $\langle\delta_a\rangle$ is the average distance between the ith event and the others in the cell,
5. If the number of the events in the cell is larger than 500 + 50, δ is decreased by δ_k
6. Points 3, 4, and 5 are repeated until the number of events in the cell is equal to 500 ± 50
7. The procedure is repeated, discarding the events already assigned to other cells, until all the events of the catalog, with a tolerance of 1%, are assigned to a cell.

The choice of 500 events represents a good one in order to obtain a stable estimation of the b value. Indeed Figure S2 in Supporting Information S1 shows that the standard deviation of the b values decreases by a factor $\simeq(3e)^{-1}$ with the number of earthquakes n_s per sample (see the Figure S2 in Supporting Information S1 caption for details) for all the catalogs here analyzed. Of course a less restrictive criterion can be applied reducing the number of earthquakes for cell when the whole number of events in the catalog is not too much large. Moreover this choice for th number of event per cell ensures, for the analyzed catalogs, a sufficiently large number of cells (Nava et al., 2017; Tramelli et al., 2021).

For all the analyzed catalogs we fix δ at 10 km. This does not affect our results at all. Indeed δ does not represents a parameter of the method, being only a starting value that has to be adjusted for reaching the wished value of the earthquake number in the cell. Similarly, k (here set at 0.1 for all the analyzed catalogs) fixes the size of the δ steps in order to obtain 500 events per cell and cannot be considered as a method parameter. k values equal to 0.05 or 0.5, for instance, would not change the results, but only the time necessary to obtain the final maps. The crucial point is that the final cell size is controlled only by the ith event and by the 500 ± 50 events not yet assigned to a cell and surrounding the ith event. Similarly the deviation ±50 (step 4) and 1% tolerance (step 6) have been introduced in order to reduce the computation time required to reach the final result. Both these values can be set equal to zero without any loss of generality.

A simple test shows that the ±50 value does not affects our results. We selected at random 20 cells for catalog, then we added to the cell 50 events selected at random from the events close to the border of the nearest cells and reevaluate m_c and b. In all cases the difference between the new and the old values of b is of the order of magnitude of the b standard deviations.

We choose to start from the largest earthquake in the catalog because this allows us to follow the spatio-temporal evolution of the seismicity. The crucial point is that the catalogs are dominated by the occurrence of aftershocks that tend to have a diffusive behavior, making space and time non independent. In this sense there is no possibility to discriminate if the difference in the b values are spatial or temporal. This characteristic is intrinsic to

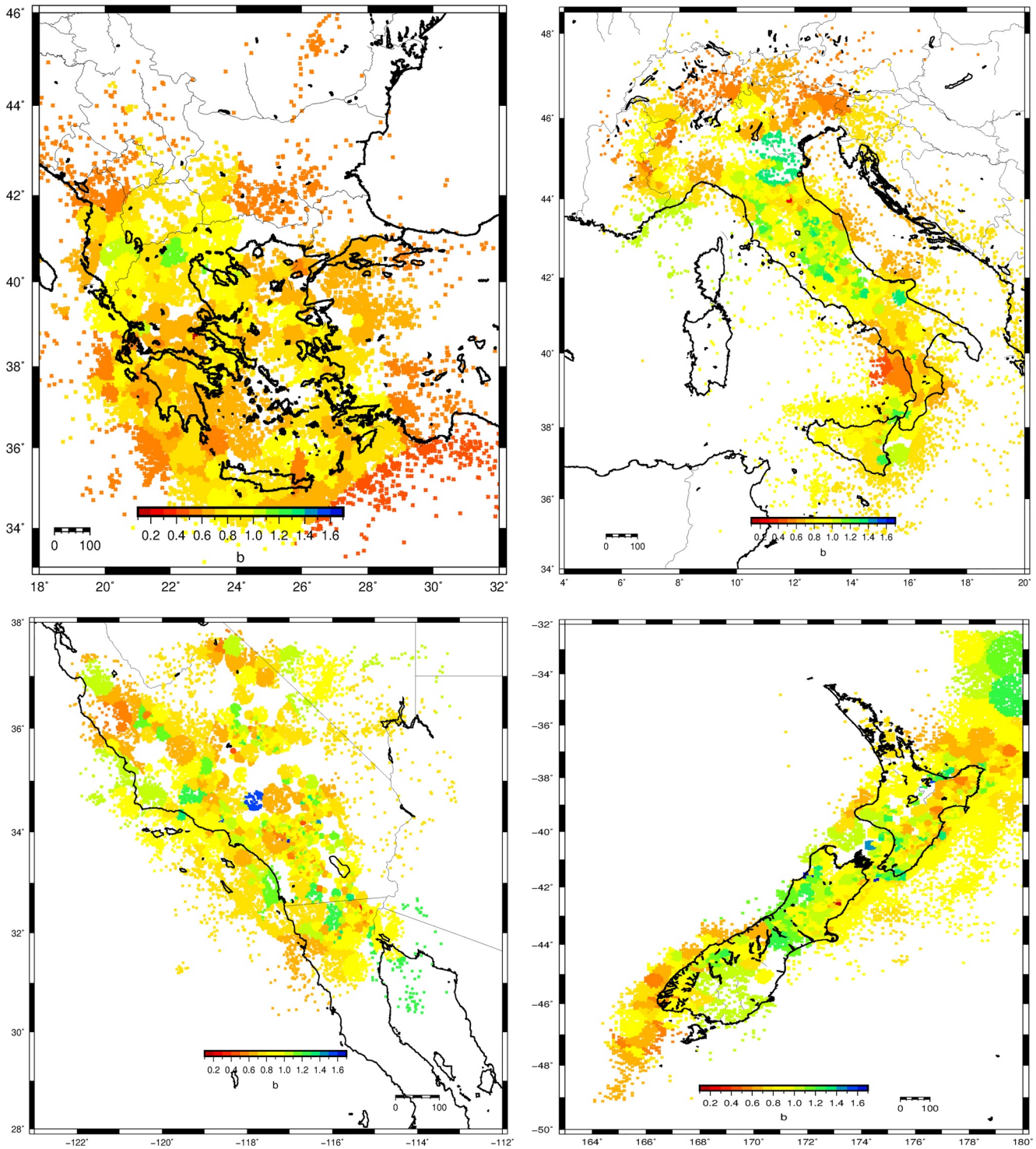

Figure 3. The map of *b* for the four catalogs here analyzed. The values are plotted only in correspondence of the earthquakes' location.

earthquake occurrence and no method can eliminate it, unless a spatial analysis of short time interval are made However this is possible only for very large sequences, for which a sufficiently large number of earthquakes per cell and per time window is available.

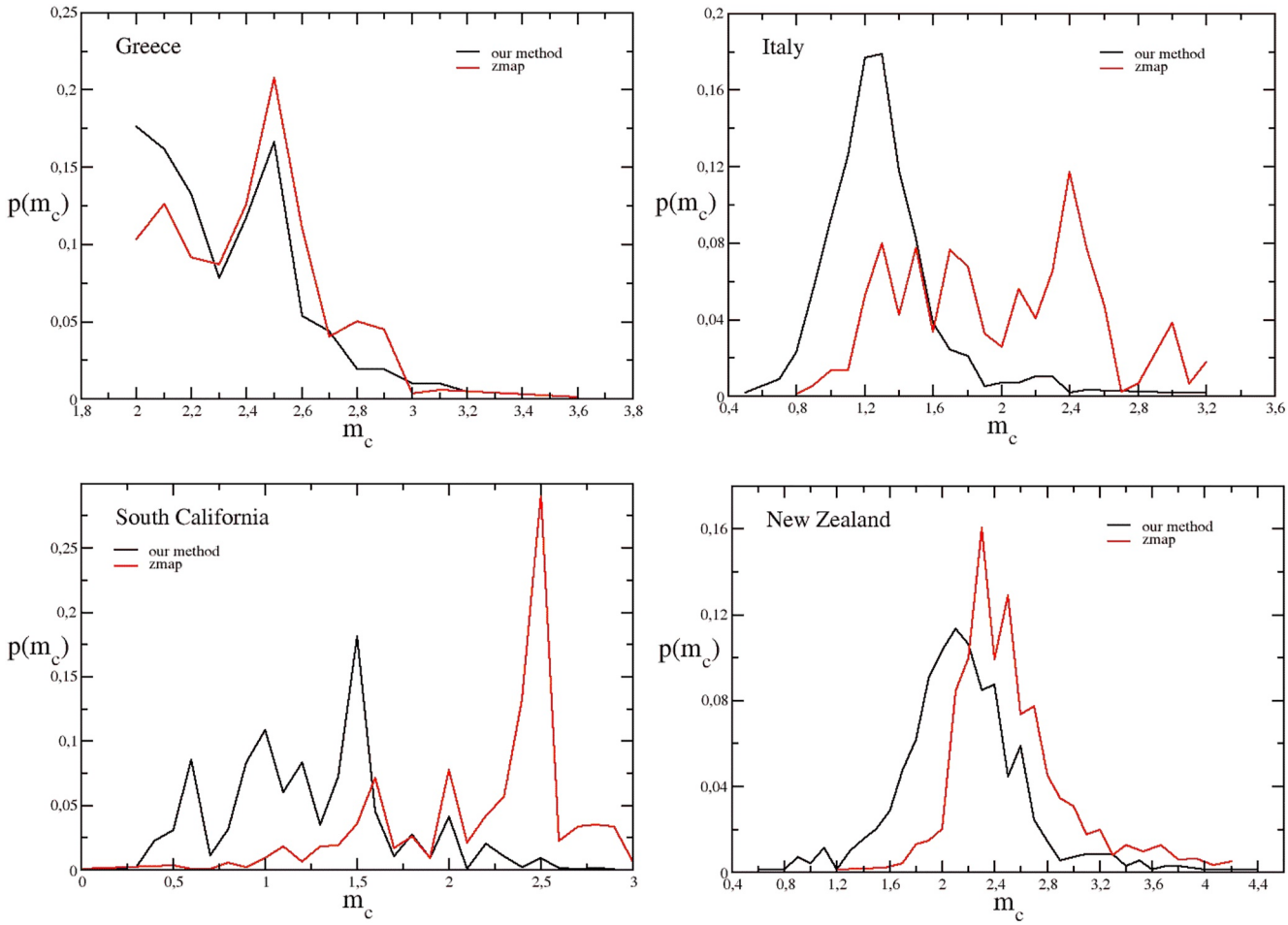

Figure 4. The normalized frequency of occurrence of m_c for the different areas here investigated compared with the ones obtained by using zmap.

Finally, a different possibility could be the use of declustered catalogs, however this will result in a smaller spatial density of earthquake, leading to a worse definition of the spatial variations of the *b* value spatial variations. This kind of analysis could be matter of future studies.

3. Results

The maps of the cells resulting for the proposed gridding method are showed in Figure 1. An intriguing observation is that the distribution the cell size (here evaluated as the average distance Δr of the earthquakes in the cell from the maximum magnitude event in the same cell) follows a power law with a very similar exponent for all the catalogs here analyzed (Figure 2; such a result implies the non-existence of a characteristic size of cells and reflects the diffusive behavior of aftershock sequences.

For each cell we estimated the completeness magnitude m_c by using the maximum curvature method (Wiemer & Wyss, 2000) in the version used by Wiemer (2001) who added 0.2 to the estimated m_c value. Although this method tends to underestimate m_c (see, among the others, Mignan and Woessner (2012)), it is very simple to implement in a code making it faster. Moreover the Gutenberg-Richter distributions are usually sharply peaked around m_c, as a consequence in many cases the estimation of m_c value could be sufficiently reliable. We remark that our focus here is on a parameter-free gridding method and this does not rely on the exact estimation of the completeness magnitude. The maps of m_c are reported in Figures S3, S4, S5, and S6 in Supporting Information S1 (also showing the maps of m_c evaluated using Zmap; see below for more details).

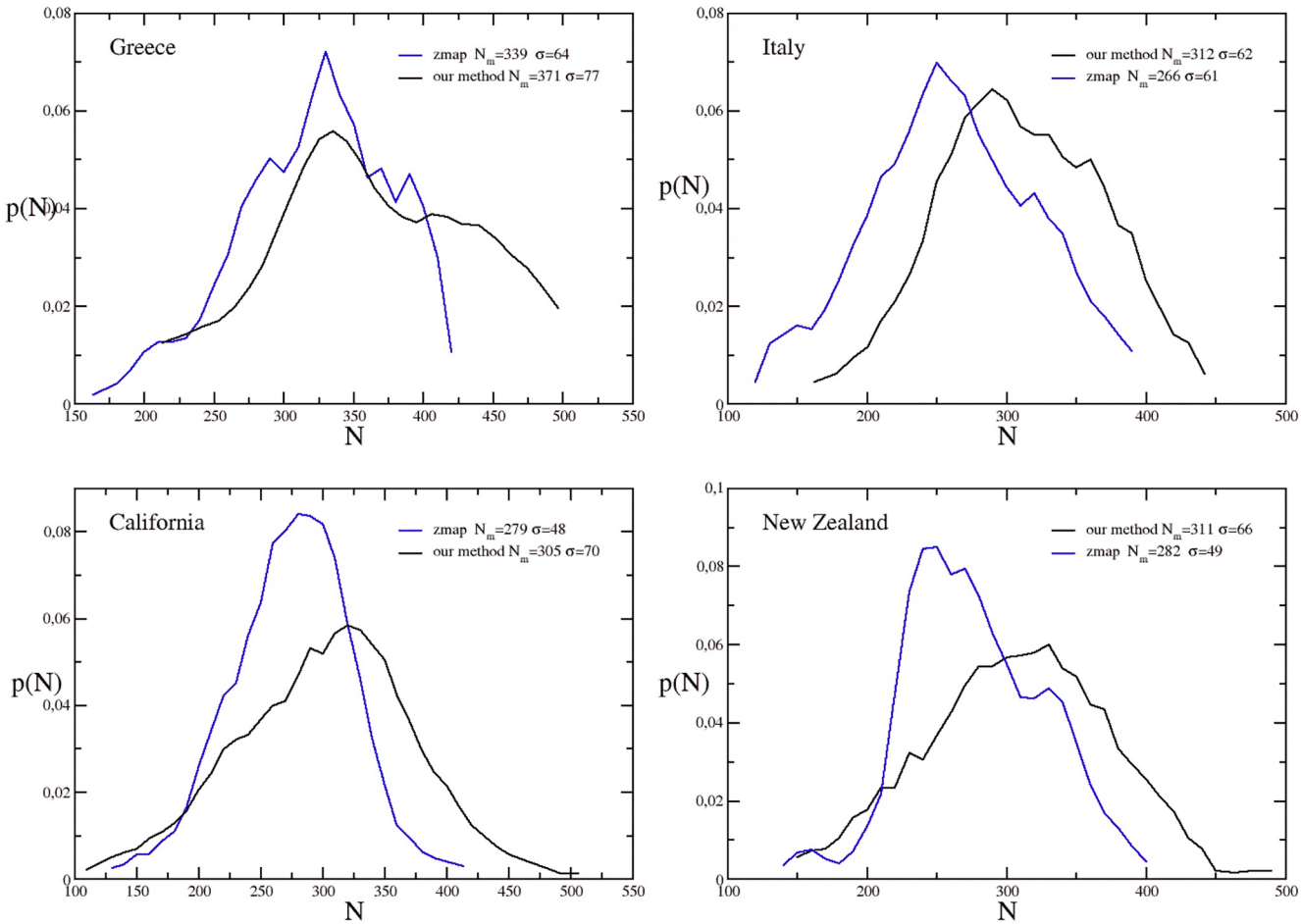

Figure 5. The distribution of the number N of earthquakes with $m \geq m_c$ in each cell and for the different areas here investigated compared with the ones obtained by using zmap.

We compute the b values only for cells verifying the condition $m_{\max} - mc \geq 2$ and uses the maximum likelihood method (Aki, 1965); whereas the estimation of the b standard deviations σ_b follows the method of Shi and Bolt (1982). The maps of b are reported in Figure 3, whereas the σ_b maps are displayed in Figures S7, S8, S9, and S10 in Supporting Information S1 where they are compared with the σ_b maps obtained with Zmap (see below for more details).

As a further test we choose an earthquake at random as the center of the cell instead of choosing the largest event in the catalog. As shown in Figure S11 in Supporting Information S1, the maps can be considered qualitatively very similar (a quantitative comparison is impossible because the cells are in principle different). This occurs because the density of aftershocks is very high close to the mainshock and, as a consequence, the probability to find the center of a cell close to the mainshock is very high. Nevertheless we prefer the not randomized version of our algorithm because it better follows the spatio-temporal evolution of the earthquake occurrence.

4. Discussions

Although here we are not interested in the exact estimation of the b value, for the sake of completeness we compare our results to ones previously obtained by other researchers. Let us to perform such a comparison area by area.

1. **Greece**: in his pioneering paper on the b value spatial variations Papazachos (1999) found that it decreases from $\simeq$1.05 to $\simeq$0.7 along a direction SE-NW, approximately parallel to the Hellenic arc. This result was confirmed by Vamvakaris et al. (2016) who used more recent data and a different and more accurate zonation.

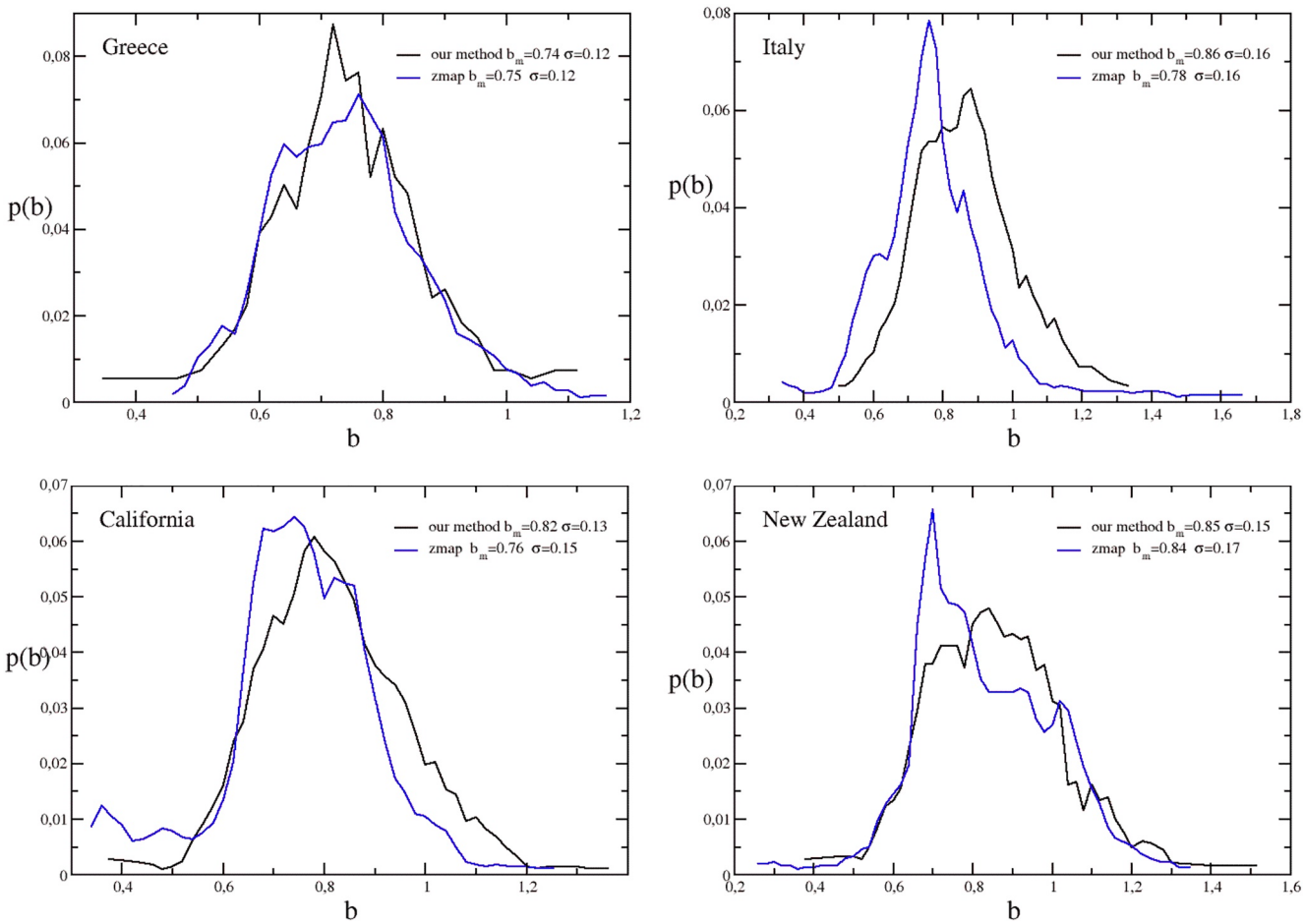

Figure 6. The distribution of the *b* values for the different areas here investigated compared with the ones obtained by using zmap.

This trend is visible also in our map (Figure 3), however the *b* variability is larger because the size of our cells is significantly smaller than those used by Papazachos (1999) and Vamvakaris et al. (2016). Moreover their *b* values are significantly larger because their m_c are larger (we are using the maximum curvature method for m_c estimation and, as well known, this method tends to underestimate m_c).

2. **Italy**: in a recent paper Taroni et al. (2021) evaluated the *b* value map for Italy by applying a modified version of the weighted likelihood approach proposed by Hu and Zidek (2002). Namely they used the Gaussian kernel already introduced by Helmstetter et al. (2007). In respect to our analysis Taroni et al. (2021) used a different catalog spanning from 1960 to 2019 (Lolli et al., 2020). In spite of these differences and of the expected greater smoothness of their map, the main result is represented by the higher *b* values in the central Apennines in the range 1.15 ÷ 1.25, interpreted either to the prevalent normal faulting of this region (Gulia & Wiemer, 2010) or to the high heat flux (Chiodini et al., 2013) associated with this region.
3. **California**: to our knowledge a detailed and complete map of the *b* values for Southern California, conputed by means of commonly used methods, does not exist for this area. Indeed, in this area, the investigation efforts have been dedicated to defining the asperities on fault segments or on plate junctions (see, among the others, the pioneering paper of Wiemer and Wyss (2002)). The only exception is represented by the investigation made by Kamer and Hiemer (2015), however the Voronoi tessellation used by these authors results into a very smooth *b* value map exhibiting *b* values in the range 0.9 ÷ 1.0. Conversely our map presents a wider range of *b* value (0.6 ÷ 1.4) with only one cell assuming the value 1.6 (outside the range) located on the locked segment of the San Andreas Fault (Lienkaemper et al., 2014).

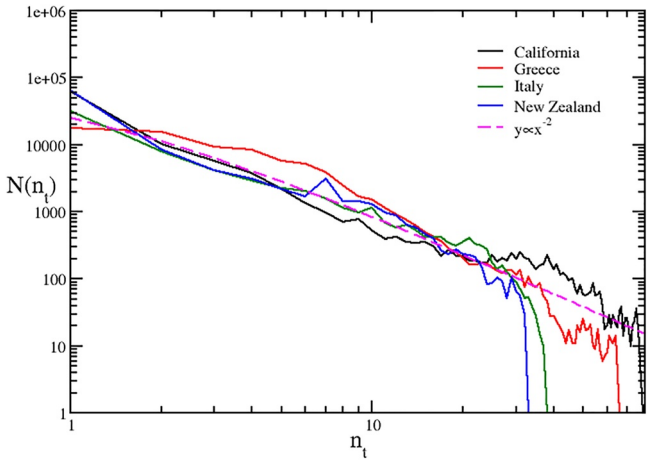

Figure 7. The distribution of the number of times n_t that an earthquake has been assigned to different cells using Zmap automatic gridding. The magenta dashed line is a power law plotted as a guide for the eyes.

4. **New Zealand**: to our knowledge, there is only a single paper presenting a b value map for the whole area (Stirling et al., 2002). The method used in this investigation to estimate the b value is based on a smoothing procedure obtaining producing smoothed maps of the b value. Moreover the authors fixed $m_c = 4$ resulting in b values significantly larger than ours. Conversely Lu (2017) obtain b values closer to our result, even if he does not present a map for the whole New Zealand and uses a shorter catalog in respect of the one used in this paper.

In the framework of our analysis, a more relevant issue is represented by the comparison of our results for the b value with those derived by using other methods. This allows a better understanding of the advantage of our parameter-free method.

We compare our results with the ones obtained using Zmap (Wiemer, 2001), probably the most used method for b maps evaluation. To this aim we used the 7.1 Zmap version. We estimated the b values using the automatic gridding suggested by the program (i.e., 41.7 km for the Italian catalog; 26.6 km for California; 26.6 km for Greece and 42.2 km for New Zealand) and, as done in our approach, the maximum curvature method to estimate m_c (Figures S2, S3, S4, and S5 in Supporting Information S1). We selected 500 nearest events within a maximum radius of 150 km. This value represents approximately the maximum Δr in the scaling regime of $p(\Delta r)$ for all the catalogs.

Figures S7, S8, S9, and S10 in Supporting Information S1 show the comparison between the maps of the b values and of σ_b obtained using our method with the ones obtained using Zmap. A visual inspection of the obtained maps reveals that the obtained b values are comparable. However, we would like to remark that in this case Zmap neglects many earthquakes. Indeed, by using the grid size automatically chosen by Zmap (see above), the 3% of the events are left out for Greece, the 44% for Italy, the 49% for California and 35% for New Zealand (the percentage refers to the number of earthquakes with $m \geq m_c$). More precisely, by *left out* we mean those events that are not used to evaluate the b value in the grid cell where they are located. It is worth to note that the same events could be used in the surrounding cell if they overlap in the same cell. This occurs because of the constant size gridding: when in a given cell the chosen number of events (here 500) is reached all the other events in the cell are left out of the analysis, reflecting into a loss of information in zones of high density of earthquake occurrence. The most important implication of this feature is a higher value of m_c, testified by its distribution (Figure 4). The only exception is represented by the Greece catalog because the left out events are a small percentage of the whole catalog. A possible explanation of a so small percentage of leaved out events for the Greece catalog is that this catalog contains only events with $m \geq 2$. Indeed the great part of the leaved out events have small magnitude even if, in principle, not smaller than m_c. In the case of our method these percentages decreases at 3.6% for California, 1.36% for Greece, 1.71% for Italy and 2.16% for New Zealand.

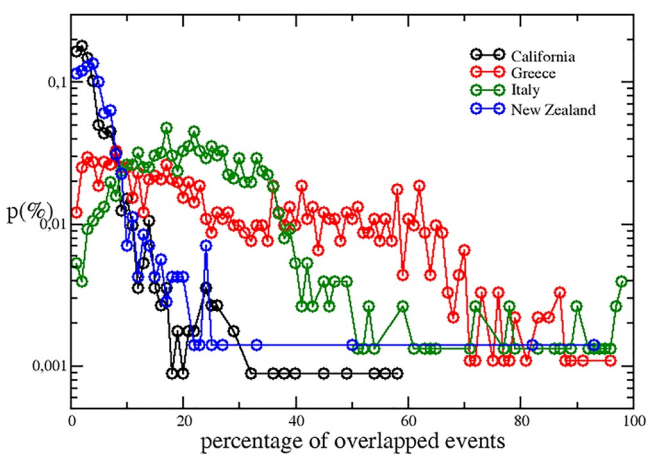

Figure 8. The distribution of the overlapped events percentage in a cell.

As a consequence, after removing the earthquakes with $m < m_c$, the number of events per cell is basically lower for the maps obtained using Zmap in respect of ones obtained with our method (see Figure 5) and the b assume lower values (see Figure 6). A χ^2 test reveals that the b value differences between the two methods cannot be considered statistically significant, however the trend is clearly enlightening that Zmap could introduce a small bias for the b values due to an overly high estimation of m_c (see Figure 4). Indeed, although both our and Zmap methods underestimate the "true" m_c value (in the sense that all the earthquakes with $m \geq m_c$ are recorded and reported in the catalog), Zmap tends to estimate higher values of m_c because of the lost earthquakes in cells of earthquake high density. It is worth to note that, for both the methods and for any region, the distributions are not centered at the commonly observed value $b = 1$. This result is due to the underestimation of m_c above mentioned, leading to an underestimation of b.

At the same time there is significant overlap in zones of low earthquakes density. Figure 7 shows $N(n_t)$ the number of times an earthquake has been assigned to n_t different cells. These distributions reveal that, for instance, 20 earthquakes are assigned to 200 different cells in in California, 1,521 earthquakes are assigned to 10 different cells in Greece, 406 earthquakes are assigned to 21 different cells in Italy and 644 earthquakes are assigned to 13 different cells in New Zealand and enlighten how important the overlapping is in zones of low earthquake density.

The degree of the overlapping is significant also after the removal of earthquakes with $m < m_c$. Figure 8 shows the distribution of the overlapped events (with $m \geq m_c$) percentage in a cell, revealing that overlapping is highly significant especially for Italy and Greece.

Of course a smaller cell size will result in a smaller number of unused events, but also in a larger overlap. Conversely a larger cell size will result in a smaller percentage of overlapping, but in a larger number of unused events. Note that there exists an obvious mutual influence between the cell size, the number of events per cell, and the maximum radius of the cell. This implies that a good compromise for these parameters is to be searched in order to obtain the smallest number of unused events and the smallest percentage of overlapping. Conversely, the use of our method does not require any search of the most convenient parameters and the number of events per cell is the only one to set.

We note that the methods weighting the contribution of earthquakes exponentially, with the spatial distance from the center of the node (Tormann et al., 2014), reasonably reduce the effects of the cells overlapping. However, these approaches evaluate b values correlated at the selected radius scale through the whole map. This makes impossible any significance test for the b values differences.

It is worth noting that the b value maps can be smoothed in order to reduce potential physical inconsistency of proximal earthquakes with different assigned b value. Indeed, for example, two earthquakes close to the border separating two different cells are assigned to two different b values, when using a not smoothed approach, in spite of their spatial proximity. However, again, smoothing introduces spatial correlations of the obtained b values making impossible any significance test for the differences.

As a final observation, we should remark that gridding the space on the basis of the largest events, or randomly choosing the center of the cell, does not guarantee the possibility of investigating of potential b variations with time, simply because the cells in different time windows are not ensured to be the same. However, still, the automated application may account for b anomalies or changes in the cell shape or disposition.

5. Conclusions

The methods commonly used for estimating the Gutenberg and Richter b-value provide distributions of this parameter over extended regions and through time. The resulting maps are suitable for deriving useful information about the seismotectonic regime and the stress variation in space and time. In general, these methods represent well established procedures and are presently widespread. However, in these classic approaches single b-values are derived by grouping earthquakes according to spatial gridding methods that, at the two extremes, implicitly produce either multiple use of a relatively large number of events (overlapping)—preventing the possibility of any statistical comparison between values obtained at distinct locations—or, if any overlap is to be avoided, exclusion of a significant number of events (omission). These two circumstances might occur at the same time to a variable extent, depending on the interplay between the grid characteristic size and the parameters set to group the earthquakes. Thus, these values should be tuned appropriately in each single application case. Based on the above observations, we considered that some different approach should be developed to group the earthquakes in order to allow statistical comparison of the estimated b-values, without waste of information. The method described here, which avoids both overlapping and the omission of the events in the catalog represents an attempt to address these issues. Also, freeing as much as possible the determination of the b value from any a-priori, ad-hoc, choice of parameters makes the proposed approach well suited for automatic applications. As discussed above, the method proposed in this study has advantages and some limitations, but likely it represents only one of several possible realizations. In this regard, this study also aims at boosting some debate, which could hopefully result in the development of further alternative methods reducing the mentioned drawbacks.

Conflict of Interest

The authors declare no conflicts of interest relevant to this study.

Data Availability Statement

Data have been provided by the Aristotele University of Thessaloniki (AUTH), the Istituto Nazionale di Geofisica e Vulcanologia (INGV), the Geological hazard information for New Zealand (GeoNet) and the Southern California Earthquake Data Center (SCEDC) and are available at the following web sites: http://geophysics.geo.auth.gr/ss/catalogs_en.html for Greece; http://terremoti.ingv.it/search for Italy; https://www.geonet.org.nz/data/types/eq_catalogue for New Zealand; scedc.caltech.edu/research-tools/altcatalogs.html for South California. All the custom codes used in this study are available at the web-site https://github.com/sismanna/b_value_map.

Acknowledgments
We would like to acknowledge the Aristotele University of Thessaloniki (AUTH), the Istituto Nazionale di Geofisica e Vulcanologia (INGV), the Geological hazard information for New Zealand (GeoNet) and the Southern California Earthquake Data Center (SCEDC) for proving the earthquake catalogue which can be downloaded at the following web sites: http://geophysics.geo.auth.gr/ss/catalogs_en.html for Greece; http://terremoti.ingv.it/search for Italy; https://www.geonet.org.nz/data/types/eq_catalogue for New Zealand; scedc.caltech.edu/research-tools/altcatalogs.html for South California. C. Godano and A. Tramelli would like to thanks the MIUR project PRIN 2017 WZFT2p for financial support. Our work was partially supported by the MIUR project PRIN 2017 WZFT2p and by Pianeta Dinamico-Working Earth INGV Project.

References

Aki, K. (1965). Maximum likelihood estimate of b in the formula log n = a − bm and its confidence limits. *Bulletin of the Earthquake Research Institute, University of Tokyo*, *43*, 237–239.

Amitrano, D. (2003). Brittle-ductile transition and associated seismicity: Experimental and numerical studies and relationship with the *b* value. *Journal of Geophysical Research*, *108*(B1), 2044. https://doi.org/10.1029/2001JB000680

Chiodini, G., Cardellini, C., Caliro, S., Chiarabba, C., & Frondini, F. (2013). Advective heat transport associated with regional Earth degassing in central Apennine (Italy). *Earth and Planetary Science Letters*, *373*, 65–74. Retrieved from https://www.sciencedirect.com/science/article/pii/S0012821X13001908 https://doi.org/10.1016/j.epsl.2013.04.009

García-Hernández, R., D'Auria, L., Barrancos, J., Padilla, G. D., & Pérez, N. M. (2021). Multiscale temporal and spatial estimation of the *b*-value. *Seismological Research Letters*, *XX*(6), 1–13. https://doi.org/10.1785/0220200388

Gulia, L., & Wiemer, S. (2010). The influence of tectonic regimes on the earthquake size distribution: A case study for Italy. *Geophysical Research Letters*, *37*(10). Retrieved from https://agupubs.onlinelibrary.wiley.com/doi/abs/10.1029/2010GL043066 https://doi.org/10.1029/2010GL043066

Gulia, L., & Wiemer, S. (2019). Real-time discrimination of earthquake foreshocks and aftershocks. *Nature*, *574*(7777), 193–199. https://doi.org/10.1038/s41586-019-1606-4

Gutenberg, B., & Richter, C. (1944). Frequency of earthquakes in California. *Bulletin of the Seismological Society of America*, *34*(4), 185–188. https://doi.org/10.1785/bssa0340040185

Helmstetter, A., Kagan, Y. Y., & Jackson, D. D. (2007). High-resolution time-independent grid-based forecast for m ≥ 5 earthquakes in California. *Seismological Research Letters*, *78*(1), 78–86. https://doi.org/10.1785/gssrl.78.1.78

Hu, F., & Zidek, J. V. (2002). The weighted likelihood. *Canadian Journal of Statistics*, *30*(3), 347–371. https://doi.org/10.2307/3316141

Kamer, Y., & Hiemer, S. (2015). Data-driven spatial b value estimation with applications to California seismicity: To b or not to b. *Journal of Geophysical Research: Solid Earth*, *120*(7), 5191–5214. https://doi.org/10.1002/2014JB011510

Lienkaemper, J. J., McFarland, F. S., Simpson, R. W., & Caskey, S. J. (2014). Using surface creep rate to infer fraction locked for sections of the San Andreas Fault system in Northern California from alignment array and GPS data. *Bulletin of the Seismological Society of America*, *104*(6), 3094–3114. https://doi.org/10.1785/0120140117

Lolli, B., Randazzo, D., Vannucci, G., & Gasperini, P. (2020). The homogenized instrumental seismic catalog (HORUS) of Italy from 1960 to present. *Seismological Research Letters*, *91*(6), 3208–3222. https://doi.org/10.1785/0220200148

Lu, S. (2017). Long-term b value variations of shallow earthquakes in New Zealand: A HMM-based analysis. *Pure and Applied Geophysics*, *174*(4), 1629–1641. https://doi.org/10.1007/s00024-017-1482-5

Mignan, A., & Woessner, J. (2012). *Estimating the magnitude of completeness for earthquake catalogs. Community online resource for statistical seismicity analysis*. https://doi.org/10.5078/corssa-00180805

Mogi, K. (1962). Study of the elastic shocks caused by the fracture of heterogeneous materials and its relation to earthquake phenomena. *Bulletin of the Earthquake Research Institute, University of Tokyo*, *40*, 125–173.

Nava, F. A., Márquez-Ramírez, V. H., Zúñiga, F. R., Ávila Barrientos, L., & Quinteros, C. B. (2017). Gutenberg-richter b-value maximum likelihood estimation and sample size. *Journal of Seismology*, *21*(1), 127–135. https://doi.org/10.1007/s10950-016-9589-1

Papazachos, C. (1999). An alternative method for a reliable estimation of seismicity with an application in Greece and the surrounding area. *Bulletin of the Seismological Society of America*, *89*(1), 111–119. https://doi.org/10.1785/bssa0890010111

Rydelek, P. A., & Sacks, I. S. (1989). Testing the completeness of Earth-quake catalogs and the hypothesis of self-similarity. *Nature*, *337*(6204), 251–253. https://doi.org/10.1038/337251a0

Scholz, C. (1968). The frequency-magnitude relation of microfracturing in rock and its relation to earthquakes. *Bulletin of the Seismological Society of America*, *58*(1), 399–415. https://doi.org/10.1785/bssa0580010399

Shi, Y., & Bolt, B. A. (1982). The standard error of the magnitude-frequency b value. *Bulletin of the Seismological Society of America*, *72*(5), 1677–1687. Retrieved from http://www.bssaonline.org/content/72/5/1677.abstract

Stirling, M. W., Verry, G. H. M., & Berryman, K. R. (2002). A new seismic hazard model for New Zealand. *Bulletin of the Seismological Society of America*, *92*(5), 1878–1903. https://doi.org/10.1785/0120010156

Taroni, M., Zhuang, J., & Marzocchi, W. (2021). High-definition mapping of the Gutenberg–Richter *b*-value and its relevance: A case study in Italy. *Seismological Research Letters*, *XX*(6), 1–7. https://doi.org/10.1785/0220210017

Tormann, T., Wiemer, S., & Mignan, A. (2014). Systematic survey of high-resolution b value imaging along Californian faults: Inference on asperities. *Journal of Geophysical Research: Solid Earth*, *119*(3), 2029–2054. https://doi.org/10.1002/2013JB010867

Tramelli, A., Godano, C., Ricciolino, P., Giudicepietro, F., Caliro, S., Orazi, M., et al. (2021). Statistics of seismicity to investigate the Campi Flegrei Caldera unrest. *Scientific Reports*, *11*(1), 7211. https://doi.org/10.1038/s41598-021-86506-6

Vamvakaris, D. A., Papazachos, C. B., Papaioannou, C. A., Scordilis, E. M., & Karakaisis, G. F. (2016). A detailed seismic zonation model for shallow earthquakes in the broader Aegean area. *Natural Hazards and Earth System Sciences*, *16*(1), 55–84. https://doi.org/10.5194/nhess-16-55-2016

Warren, N. W., & Latham, G. V. (1970). An experimental study of thermally induced microfracturing and its relation to volcanic seismicity. *Journal of Geophysical Research*, *75*(23), 4455–4464. https://doi.org/10.1029/JB075i023p04455

Wiemer, S. (2001). A software package to analyze seismicity: ZMAP. *Seismological Research Letters*, *72*(3), 373–382. https://doi.org/10.1785/gssrl.72.3.373

Wiemer, S., McNutt, S. R., & Wyss, M. (1998). Temporal and three-dimensional spatial analyses of the frequency–magnitude distribution near Long Valley caldera, California. *Geophysical Journal International*, *134*(2), 409–421. https://doi.org/10.1046/j.1365-246x.1998.00561.x

Wiemer, S., & Wyss, M. (1997). Mapping the frequency-magnitude distribution in asperities: An improved technique to calculate recurrence times? *Journal of Geophysical Research*, *102*(B7), 15115–15128. https://doi.org/10.1029/97jb00726

Wiemer, S., & Wyss, M. (2000). Minimum magnitude of completeness in earthquake catalogs: Examples from Alaska, the Western United States, and Japan. *Bulletin of the Seismological Society of America*, *90*(4), 859–869. https://doi.org/10.1785/0119990114

Wiemer, S., & Wyss, M. (2002). Mapping spatial variability of the frequency-magnitude distribution of earthquakes. *Advances in Geophysics*, *45*, 259–302.

Wyss, M. (1973). Towards a physical understanding of the earthquake frequency distribution. *Geophysical Journal of the Royal Astronomical Society*, *31*(4), 341–359. https://doi.org/10.1111/j.1365-246X.1973.tb06506.x

Wyss, M., Shimazaki, K., & Wiemer, S. (1997). Mapping active magma chambers by b values beneath the off-Ito volcano, Japan. *Journal of Geophysical Research*, *102*(B9), 20413–20422. https://doi.org/10.1029/97JB01074